Carbon nanotube Josephson junctions with Nb contacts

E. Pallecchi,[1,a] M. Gaaß,[1] D. A. Ryndyk,[2] and Ch. Strunk[1]
[1]*Institute for Experimental and Applied Physics, University of Regensburg, D-93040 Regensburg, Germany*
[2]*Institute for Theoretical Physics, University of Regensburg, D-93040 Regensburg, Germany*

(Received 27 March 2008; accepted 27 July 2008; published online 18 August 2008)

We report on the preparation of carbon nanotube Josephson junctions using superconducting electrodes made of niobium. Gate-controllable supercurrents with values of up to 30 nA are induced by the proximity effect. The *IV* curves are hysteretic at low temperature and the corresponding switching histograms have a width of 0.5%–2%. An on-chip resistive environment integrated in the sample layout is used to increase the switching current. © *2008 American Institute of Physics*. [DOI: 10.1063/1.2971034]

A Josephson junction is characterized by a phase coherent transfer of Cooper pairs across a weak link between two superconducting electrodes.[1,2] Such a weak link can be formed by a thin insulating layer, a short bridge of normal conducting material, or even a single atom.[3] A central application of Josephson junctions is the so-called superconducting quantum interference device (SQUID). These devices are widely used as flux sensors with sensitivities of up to $10^{-6}\Phi_0$ which, for typical geometries, corresponds to a magnetic field as low as 10^{-15} T.[4] The use of SQUID magnetometry runs into limitations for magnetic nanoclusters or single molecule magnets,[5] where only a very small fraction of magnetic flux couples into the pickup loop of the SQUID. For such small systems, the use of single-wall carbon nanotubes (SWNTs) or multiwall carbon nanotubes (MWNTs) as weak links for the SQUID is a promising way for a considerable improvement.[6,7] Proximity induced supercurrent has been reported in ropes and individual carbon nanotubes mainly with aluminum contacts.[6–10] It has been suggested that a stronger proximity effect and therefore a more efficient SQUID could be realized by using niobium[7] since it can be operated in a wider temperature and magnetic field range.

In this letter, we report on the fabrication and measurement of a niobium-MWNT-niobium Josephson junction. We performed our measurement in a dilution refrigerator with a base temperature of 25 mK. To observe expected critical currents of only a few nanoamperes a proper filtering scheme is essential. We used a combination of room temperature (π-filters) and low temperature (copper powder and *RC* filters) filtering, which covers all the frequency range above 10 kHz. Moreover, highly resistive ($R_\square \simeq 21\ \Omega$) AuPd leads provide damping at the plasma frequency of the junction,[11] while the bonding pads of the sample form the necessary capacitors. An image of a typical sample is shown in Fig. 1(a).

High purity arc-discharge grown MWNTs with 10 nm diameter are deposited onto a highly doped silicon wafer with a 400 nm thick thermal oxide layer. A four-point lead configuration was patterned by standard electron beam lithography and thermal evaporation of 5 nm of Ti as an adhesion layer followed by 40 nm of AuPd. The Nb contacts were prepared in a second lithography step by evaporating first a 3 nm thin palladium interlayer to improve the contact transparency, followed by sputtering 45 nm of niobium in the same UHV run. For a Nb/Pd bilayer of similar geometry, we measured a transition temperature of $T_C = 7.5$ K.

Typical room temperature resistances of our devices are in the range of 5–10 kΩ. In Fig. 1(b), we present electric transport data taken at $T = 25$ mK with a fixed bias current of $I_{\text{bias}} = 0.5$ nA. For gate voltages V_g above about −8 V, the conductance is rather low ($G < 15\ \mu$S) with a transition to nearly equidistant Coulomb peaks above −4 V ($G < 3\ \mu$S). For $V_g \lesssim -8$ V, the resistance remains below 20 kΩ and drops to zero in certain regions. For $V_G \lesssim -12$ V the sample remains superconducting. At low temperatures the current-voltage (*IV*) characteristics of the devices show hysteretic switching from a zero or low resistance to a high resistance state as the bias current exceeds a certain value I_{SW}. At $T = 25$ mK, the switching current $I_{\text{SW}}(V_G)$ varies with the gate voltage and shows, on average, a clear tendency to increase as V_G is tuned more negative. Superimposed on the increasing background, we observe a resonant modulation of I_{SW}. At

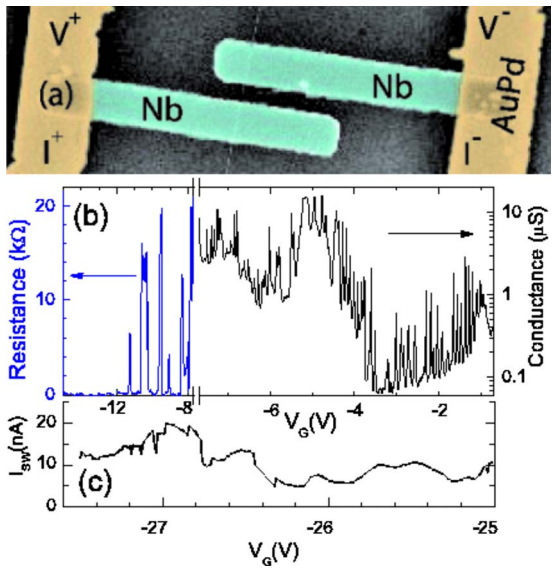

FIG. 1. (Color online) (a) SEM image of a typical sample from this work. The spacing between the Nb contacts to the MWNT is 350 nm. The Nb contacts are connected to resistive AuPd leads. (b) Transition from a high transparency regime at negative gate voltage V_G (left) with partially vanishing resistance (blue) to a Coulomb blockade regime with partially vanishing conductance (black) at more positive V_G (right). (c) Switching current $I_{\text{SW}}(V_G)$ at more negative gate voltage.

[a]Electronic mail: emiliano.pallecchi@gmail.com.

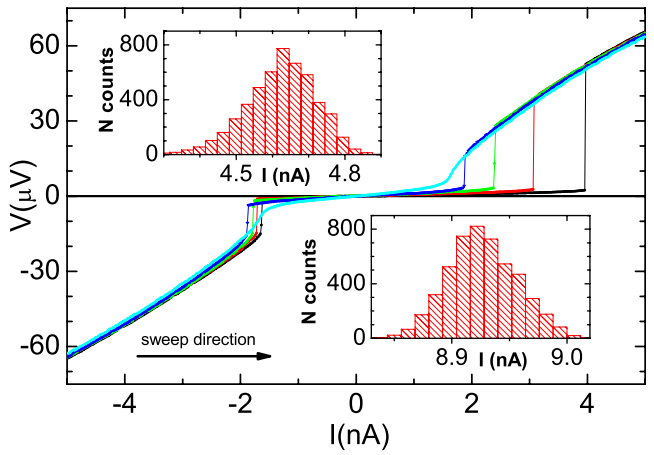

FIG. 2. (Color online) *IV* characteristics measured at $V_G=-22.3$ V, the arrow indicates the sweep direction. The first jump at negative currents of each *IV* corresponds to the retrapping current, while the one at positive current is the switching current. Different colors correspond to different temperatures, from 200 mK (highest switching current) to 600 mK (lowest switching current) in steps of 100 mK. The insets show two switching histograms with 5000 sweeps each, measured at $V_G=-22.3$ V, $T=125$ mK (up left) and $V_G=-24.3$ V, $T=50$ mK (down right).

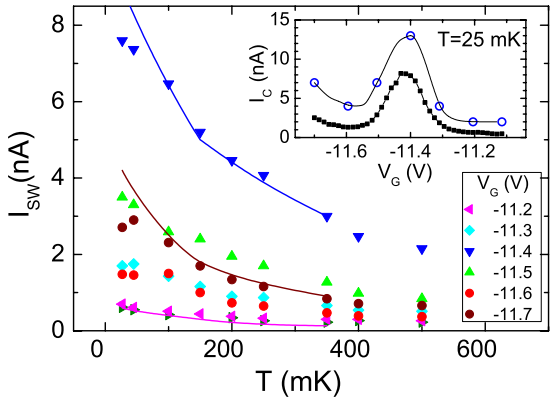

FIG. 3. (Color online) Temperature dependence of the switching current for different gate voltages. The solid line is a fit to the data obtained from the thermal fluctuation theory. The inset shows the measured switching current (solid dots) together with the values of the intrinsic critical current I_C extracted from the fits.

high negative gate voltage, we observed sudden changes of the normal state resistance R_N and the switching current I_{SW} indicating the motion of trapped charges in the silicon oxide Fig. 1(c). In the range $-32\ \text{V}<V_G<+32\ \text{V}$, we found a maximum of $I_{SW}=31$ nA, which is high compared to earlier reports on MWNTs.[10] This behavior is consistent with an increase of the transparency of the contacts at negative gate voltages, as previously observed in Nb-SWNT-Nb junctions.[12] The rather high value of the switching current can be attributed to several factors such as the on-chip electromagnetic environment, which reduces the switching of the Josephson junction and the high transparency junctions.

We also checked the stability of our junction against thermal cycling and aging. We cooled down the sample a total of five times over a period of almost six months. It was always possible to identify the two characteristic V_G regions corresponding to Coulomb blockade and supercurrent, approximately in the same gate range. Slight differences in gate voltage range at consecutive cooldowns can be explained by changes of the extrinsic doping level.

In Fig. 2, we plot the *IV* characteristics for different temperatures at $V_G=-24.3$ V, recorded at the third cooldown, where current has been swept from minus to plus. At low temperature, the curves show hysteretic switching while, when increasing the temperature, the hysteresis is gradually suppressed. The retrapping current, i.e., the current at which the junction switches back from the normal into the superconducting state, is much less temperature dependent and decreases when the temperature is decreased. Already prior to the switch of the junction from the superconducting to the quasiparticle branch, the resistance becomes finite as expected for an overdamped junction with phase diffusion. The hysteretic switching and the phase diffusion can coexist provided that the damping at the plasma frequency is sufficiently strong.[13,14]

In Fig. 3, we present the temperature dependence of the critical current for different gate voltages at the same resonance. At 300 mK and $V_G=-11.5$ V, we still find a sizable switching current of $I_{SW}\simeq 4$ nA, which greatly facilitates sensor applications. We further studied the statistics of the switching by repeating 5000 *IV* sweeps and recording the switching current for each of them. Two examples are plotted in the insets of Fig. 2. We measured a typical full width at half maximum of 0.5%–2% at 50 mK.

For the physical interpretation of the data, it is important to note that observed temperature dependent switching current can be very different from the intrinsic $I_C(T)$ curve of the junction in absence of thermal fluctuations.[15] Using a T-independent I_C as single fit parameter, we calculated $I_{SW}(T)$ with the help of an extended resistively shunted junction (RSJ) model[16] containing thermal current noise and the coupling to an external *RC* circuit, which accounts for our on-chip electromagnetic environment.

The solid lines in Fig. 3 have been obtained using the measured junction resistance after the switch, the resistance of the external $R_{ext}=350\ \Omega$, and $C=11.5$ pF –the external capacitance. The capacitance of the Josephson junction is estimated as $C_J\approx 0.2$ fF, which can be neglected. The importance of fluctuations is quantified by the parameter $\gamma=2ek_BT/\hbar I_C\simeq 0.044T[\text{mK}]/I_C[\text{nA}]$ (k_B is the Boltzmann constant). The crossover temperature T^* between the strong ($\gamma>1$) and the weak ($\gamma<1$) regime is determined by the condition $E_J(T^*)\simeq k_BT^*$, where $E_J(T)=\hbar I_C(T)/2e$ is the Josephson coupling energy. It is thus clear that in our experiments, we operate the crossover region $\gamma\simeq 1$. The agreement between the measured T dependence of the I_{SW} with the model (solid line in Fig. 3) is good, except at $T<100$ mK, where the observed I_{SW} is slightly reduced. In the inset, we plot the switching current at 25 mK measured along the resonance and the corresponding critical currents extracted using the model described.

In the evolution of the current-voltage characteristics, three temperature regimes can be distinguished. At low temperatures, $T\ll T^*$ the voltage in the superconducting state is negligible and we observe hysteretic switching to the high resistance branch and back. At temperature $T\sim T^*$, the current voltage curves display a small but finite voltage below the switching current (phase-diffusion branch), but switching is still present. At high temperatures $T>T^*$, the *IV* curves are smooth without jumps. The critical current is indicated by the maximal curvature of $I(V)$.

When taking into account the effects of fluctuations, no intrinsic T dependence of the critical current remains in the investigated range of temperatures. This indicates that the energy scales controlling the latter exceed 50 μV. In fact, both the energy gap of the Nb Δ and the Thouless energy E_{Th} of the nanotube are of the order of 1 mV, i.e., more than an order of magnitude larger. What is the reason for the resonant variation of I_C? Although MWNTs are usually disordered, the Coulomb blockade patterns are rather regular in this sample. The Coulomb diamonds close at low bias voltage (not shown), indicating that disorder does not split the tube into several weakly coupled quantum dots as in other cases (in particular for tubes with larger diameter). The spacing of the Coulomb peaks is very even and resembles that of metallic islands with little evidence of a finite level spacing. This may be attributed to the availability of states in the inner shells of the tubes. The supercurrent resonances are accompanied by weaker transmission resonances in the normal state conductance at high magnetic fields ($\simeq$6 T). It is likely that both are produced by constructive quantum interference of the underlying single particle states, which in presence of weak disorder is more of a conductance fluctuation type rather than regular Fabry–Pérot oscillations.[8] At strongly negative gate voltages, the overall contact transparency becomes very high, leading to a lifetime broadening of the resonances, which exceeds their distance. For this reason, the supercurrent remains substantial between the resonance peaks.

In conclusion, we have realized a Josephson junction with a MWNT as weak link and niobium as superconductor. The value of the critical current could be widely tuned by applying a gate voltage. At positive gate voltages, the supercurrent was suppressed and the transport was dominated by Coulomb blockade. At negative gate voltage, we observed critical currents up to a value of 30 nA. The junction properties are reproducible in successive cooldowns and stable in time. Thanks to the use of niobium, the critical current is robust against temperature and magnetic field, making it suitable for future application in nano-SQUIDs.

We thank L. Forro and C. Miko for providing the carbon nanotubes and T. Novotny and C. Urbina for fruitful discussions. This work was supported by the EU FP6 CARDEQ project and by the Graduiertenkolleg GK638.

[1] B. D. Josephson, Phys. Lett. **1**, 251 (1962).
[2] K. K. Likharev, Rev. Mod. Phys. **51**, 101 (1979).
[3] M. F. Goffman, R. Cron, A. Levy Yeyati, P. Joyez, M. H. Devoret, D. Esteve, and C. Urbina, Phys. Rev. Lett. **85**, 170 (2000).
[4] *The SQUID Handbook*, edited by J. Clarke and A. I. Braginski (Wiley, Weinheim, 2004).
[5] W. Wernsdorfer, Adv. Chem. Phys. **118**, 99 (2001).
[6] A. Kasumov, M. Kociak, M. Ferrier, R. Deblock, S. Guéron, B. Reulet, I. Khodos, O. Stéphan, and H. Bouchiat, Phys. Rev. B **68**, 214521 (2003).
[7] J. P. Cleuziou, W. Wernsdorfer, V. Bouchiat, T. Ondarcuhu, and M. Monthioux, Nat. Nanotechnol. **1**, 53 (2006).
[8] P. Jarillo-Herrero, J. A. van Dam, and L. P. Kouwenhoven, Nature (London) **439**, 953 (2006).
[9] H. I. Jørgensen, K. Grove-Rasmussen, T. Novotný, K. Flensberg, and P. E. Lindelof, Phys. Rev. Lett. **96**, 207003 (2006); H. I. Jørgensen, T. Novotný, K. Grove-Rasmussen, K. Flensberg, and P. E. Lindelof, Nano Lett. **7**, 2441 (2007).
[10] T. Tsuneta, L. Lechner, and P. Hakonen, Phys. Rev. Lett. **98**, 087002 (2007).
[11] J. M. Martinis and R. L. Kautz, Phys. Rev. Lett. **63**, 1507 (1989).
[12] A. Morpurgo, J. Kong, C. M. Marcus, and H. Dai, Science **286**, 263 (1999).
[13] D. Vion, M. Goetz, P. Joyez, D. Esteve, and M. H. Devoret, Phys. Rev. Lett. **77**, 3435 (1996).
[14] M. Tinkham, *Introduction to Superconductivity* (McGraw-Hill, Singapore, 1996).
[15] T. A. Fulton and L. N. Dunkleberger, Phys. Rev. B **9**, 4760 (1974).
[16] R. L. Kautz and J. M. Martinis, Phys. Rev. B **42**, 9903 (1990).